Current Cardiovascular Imaging Reports (2021) 14: 5
https://doi.org/10.1007/s12410-021-09555-5

CARDIAC NUCLEAR IMAGING (A. CUOCOLO AND M. PETRETTA, SECTION EDITORS)

40 Years Anniversary of Cardiac ^{123}I-*m*IBG Imaging: State of the Heart

D. O. Verschure[1,2] · K. Nakajima[3] · A. F. Jacobson[4] · H. J. Verberne[1]

Accepted: 3 July 2021 / Published online: 3 September 2021

Abstract

Purpose of Review This narrative review reflects on the body of evidence on cardiac ^{123}I-*m*IBG imaging that has accumulated since the introduction in the late 1970s and focusses on to what extent cardiac ^{123}I-*m*IBG imaging has fulfilled its potential in cardiology especially.

Recent Findings In contrast to the linear relationship between ^{123}I-*m*IBG-derived parameters and overall prognosis in heart failure, there seems a "bell-shape" curve for ^{123}I-*m*IBG-derived parameters and arrhythmic events. In addition, there is a potential clinical role for cardiac ^{123}I-*m*IBG in optimizing patient selection for expensive devices (i.e., ICD and CRT). This needs of course to be established in future trials.

Summary Cardiac ^{123}I-*m*IBG imaging is, despite the numerous of studies, sometimes mistakenly seen as a nice to have technique rather than a must have imaging modality. Although cardiac ^{123}I-*m*IBG imaging has grown and matured over the years, its full clinical potential has still not been tested to the maximum.

Keywords Chronic heart failure · ^{123}I-*m*IBG scintigraphy · Heart-to-mediastinum ratio · Washout · Prognosis

Introduction

Meta-iodobenzylguanidine (*m*IBG), an analog of the false neurotransmitter guanethidine, was developed in the late 1970s as an agent for imaging of the adrenal medulla [1]. However, even in the earliest work with this compound, its potential for use in assessing the autonomic nervous system of the heart in terms of uptake and retention of a norepinephrine (NE) analog was noted [1]. In fact, within months of the first publication of successful ^{131}I-*m*IBG adrenal imaging in dogs, animal and human images of the heart were reported [2, 3]. In the latter report, five male volunteers (ages 23–31) underwent a series of images of the chest in the left anterior oblique projection during the first 2 h after administration of 74 MBq of ^{123}I-*m*IBG. In all cases, the left ventricular myocardium was visualized by 2 min. These studies mark the start of the odyssey to discover clinical applications for imaging of myocardial sympathetic innervation.

In the decade following the initial reports on cardiac ^{123}I-*m*IBG imaging, numerous investigators in the United States of America (USA), Europe, and Japan examined the potential of this procedure in a variety of cardiac disease populations. The early observation of an inverse relationship between circulating catecholamine plasma levels and cardiac uptake of *m*IBG raised the possibility that *m*IBG imaging in other diseases with adrenergic dysfunction and/or increased circulating catecholamine levels, such as heart failure (HF), might be of clinical value [4–6]. Decreased myocardial uptake of ^{123}I-*m*IBG was reported in patients with cardiomyopathy [7, 8] and in patients following acute myocardial infarction [9]. A large prospective trial of cardiac ^{123}I-*m*IBG imaging, performed in Japan in the late 1980s [10], showed good image quality for planar and single photon emission computed tomography (SPECT) ^{123}I-*m*IBG imaging in a variety of patients with known ischemic heart disease. Alone and in comparison to thallium-201 myocardial perfusion imaging

This article is part of topical collection on *Cardiac Nuclear Imaging*

✉ D. O. Verschure
d.o.verschure@amsterdamumc.nl

[1] Department of Radiology and Nuclear Medicine, Amsterdam UMC, Location AMC, University of Amsterdam, Meibergdreef 9, 1105AZ, Amsterdam, The Netherlands

[2] Department of Cardiology, Zaans Medical Centre, Zaandam, The Netherlands

[3] Department of Functional Imaging and Artificial Intelligence, Kanazawa University Hospital, Kanazawa, Japan

[4] Diagram Consulting, Hawaii, USA

(MPI), the large majority of over 800 patients in the study had ^{123}I-*m*IBG images that were interpretable for assessment of sympathetic innervation.

The earliest investigations of cardiac ^{123}I-*m*IBG imaging relied primarily on qualitative or semi-quantitative measures of uptake, either alone or in combination with MPI studies [5, 10]. However, within a few years, analyses based on pixel- and voxel-based activity determinations on planar and SPECT images were used to characterize neuronal dysfunction associated with various cardiac diseases. In the absence of absolute quantitation techniques, it became common practice to compare heart (H) uptake with activity in adjacent regions such as the lungs (L) and mediastinum (M) [8, 11]. The heart-to-mediastinum (H/M) ratio soon became a commonly used descriptor of cardiac ^{123}I-*m*IBG uptake on both planar and SPECT images [7, 8, 12].

Another measure of cardiac adrenergic integrity, "^{123}I-*m*IBG washout" (WO), was developed as a result of use of multiple time-point imaging during the early investigations of this imaging agent. Calculation of the change in cardiac activity between early (typically 15–30 min post-injection) and late (3–4 h post-injection) images demonstrated a significant difference between normal and abnormal hearts, with more rapid loss of activity associated with disease [7, 11, 13]. The early H/M ratio predominantly reflects the integrity of sympathetic nerve terminals (i.e., number of functioning nerve terminals and intact uptake-1 mechanism (norepinephrine transporter)). The late H/M ratio particularly offers information about neuronal function resulting from uptake, storage, and release. The ^{123}I-*m*IBG WO reflects predominantly neuronal integrity of sympathetic tone/adrenergic drive [14].

As experience with ^{123}I-*m*IBG cardiac imaging increased, the number of patients studied became sufficient to allow assessment of the prognostic significance of the findings on these studies over time. The first major report, published in 1992, used multivariate stepwise regression discriminant analysis to demonstrate that the H/M ratio was a stronger predictor of survival probability than other indices (x-ray cardiothoracic ratio, echographic end-diastolic diameter, and radionuclide left ventricular ejection fraction) in patient with cardiomyopathy followed for 1–27 months [15]. This observation has since been confirmed in multiple subsequent retrospective and prospective studies, some of which are described later in this review. There is now 30 years of evidence of the prognostic value of ^{123}I-*m*IBG cardiac imaging, particularly in patients with ischemic and non-ischemic heart failure. More generally, cardiac ^{123}I-*m*IBG imaging has been established as a highly reproducible [16–18] and feasible technique to evaluate and assess any disease that results in autonomic dysfunction affecting the heart.

Cardiac ^{123}I-*m*IBG Imaging Acquisition and Analyses

Both planar and SPECT cardiac ^{123}I-*m*IBG imaging have been widely used to evaluate global and regional cardiac sympathetic function. A standard dose of ^{123}I-*m*IBG varies among countries: 111 MBq in Japan, 185 MBq in Europe, and 370 MBq in the USA. After administration of ^{123}I-*m*IBG early (15–30 min) and late (3–4 h), images are acquired using a gamma camera equipped with a low-energy (LE) or medium-energy (ME) collimator. Typical acquisition conditions for planar and SPECT images are summarized in Table 1. Among several quantitation methods, the H/M ratio and ^{123}I-*m*IBG WO has been most widely used in cardiology and neurology applications. This method is based on a simple ratio of average counts (count/pixel) of the heart and mediastinum [19••]. The regions of interest (ROI) are set as a cardiac contour, ellipsoid or circle on the heart and a fixed rectangular shape on the upper mediastinum [16, 20, 21] (Figure 1). There are variations to the WO (%) calculation using the myocardial count densities only, requiring a time-decay correction (factor of 1.21*), without (B) or with background correction (C):

$$\text{(A)}\quad \mathrm{WO} = \left\{\frac{(\text{early H/M ratio} - \text{late H/M ratio})}{\text{early H/M ratio}}\right\} * 100$$

$$\text{(B)}\quad \mathrm{WO} = \left\{\frac{(\text{early H}) - (\text{late H} * 1.21)}{\text{early H}}\right\} * 100$$

$$\text{(C)}\quad \mathrm{WO} = \left\{\frac{(\text{early H-early M}) - (\text{late H-late M}) * 1.21}{(\text{early H-early M})}\right\} * 100$$

* = ^{123}I decay correction for 3 h and 45 min (1: 0.8213).

Normal ranges for H/M ratios and WO have been derived from normal databases to standardize definition of abnormal thresholds for various camera-collimator types and possibly for different populations. Japanese normal databases have defined the normal ranges of early (20 min) and late H/M ratios (3 h) of 2.2–4.0 and 2.3–4.4, respectively. Upper limit of ^{123}I-*m*IBG WO is 34% if calculated by heart count with background and time-decay corrections (equation C) and 14% if calculated by the formula in equation A [22, 23].

Compared with the H/M ratio derived from two-dimensional planar images, the results of three-dimensional imaging using SPECT provide a more complete understanding of global innervation. The SPECT acquisitions are comparable with MPI. Analysis can be performed similar to the 17-segment/5-point model used for MPI [24]. An example is shown in Figure 2.

A normal database for ^{123}I-*m*IBG SPECT imaging has also been developed by the Japanese Society of Nuclear Medicine working group [22]. Although this specific database cannot be applied to patients with markedly impaired cardiac

Table 1. Recommended cardiac ^{123}I-*m*IBG imaging acquisition conditions.

Pre-test treatment	Medications: discontinue medications to interfere norepinephrine uptake Thyroid blockade: (optional; may not necessarily be used)
Administration dose	111–370 MBq (3–10 mCi)
Timing of acquisition	15–30 min (early) and 3–4 h (late) post-injection
Planar image	At least anterior image
	128 × 128 or 256 × 256 matrix
	5–10 min
	LE or ME collimators (standardization recommended)
SPECT image	64 × 64 matrix
	3–6-degree step, 30 s per projection*
	180- or 360-degree rotation
	*Total acquisition time adjusted for 20–30 min with Anger camera, and 10 min with cardiac CZT camera

sympathetic activity, use of such standard databases facilitates evaluation of ^{123}I-*m*IBG images. Without access to these databases, careful visual evaluation is essential, incorporating the specific distribution patterns of cardiac ^{123}I-*m*IBG. Furthermore, comparison of cardiac SPECT ^{123}I-*m*IBG images with MPI can also be useful in specific cardiac pathologies such as ischemic heart disease. However, the combined assessment of myocardial innervation and perfusion has not been gained wide implementation, possibly due to relatively higher radiation exposure and long acquisition time. In the last two decades, solid-state cardiac cameras with CTZ detector have been developed that allow the assessment of myocardial innervation and perfusion in a single imaging session with limited radiation exposure and acquisition time [25, 26].

Standardization

Although a large number of studies on planar ^{123}I-*m*IBG assessed cardiac sympathetic activity have been published, methodological and analytical limitations have hampered wide-scale clinical implementations of cardiac ^{123}I-*m*IBG scintigraphy and also hampered comparison between different institutions. Moreover, most of these data are acquired from single center experiences and do not necessarily allow extrapolation of the obtained results to other institutions. Essential for large-scale implementation of cardiac ^{123}I-*m*IBG imaging is adequate reproducibility, standardization, and validation as suggested by Flotats et al. [19]. Furthermore, the American

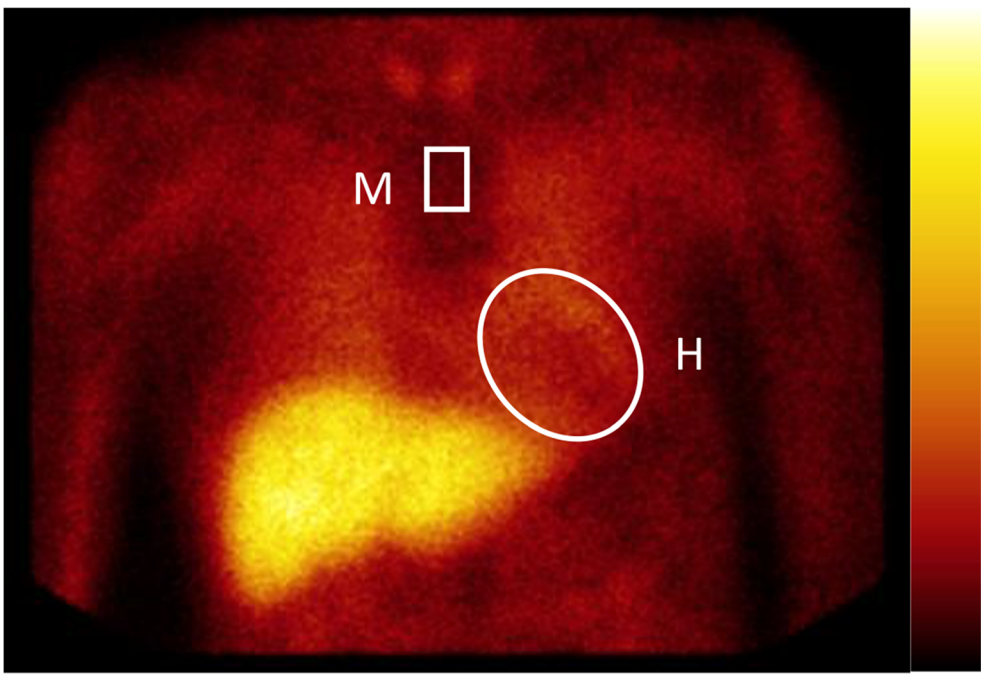

Figure 1. Example of placing a region of interest (ROI) over the heart (H) and fixed rectangular mediastinal ROI placed on the upper part of the mediastinum (M) for calculating H/M ratio.

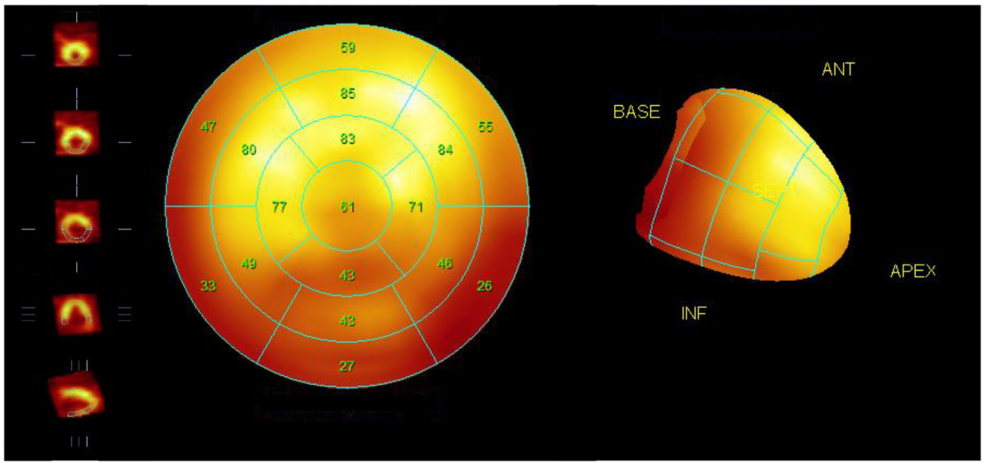

Figure 2. Example of late ^{123}I-*m*IBG SPECT imaging. On the left, the conventional short, vertical, and horizontal axis; in the middle, the corresponding 17-segment model polar map, and on the right, a 3D reconstruction. There is impaired regional ^{123}I-*m*IBG uptake in the inferior wall from the myocardial base until the apex with extension to both inferoseptal and inferolateral regions.

Society of Nuclear Cardiology (ASNC) recommends locations of heart (heart shape) and mediastinum (7 × 7 pixels) [27], and Japanese semi-automatic software (smartMIBG) uses a template of circular cardiac region and rectangular mediastinal region (30% of the mediastinal height, and 10% of the width) [28].

Due to a non-negligible fraction of scatter and collimator septal penetration from ^{123}I high-energy photons, variation in H/M ratio have been problematic, particularly when results from LE and ME collimators were mixed [29]. Among several methods applied, a calibration phantom-based correction method for different collimator and gamma cameras has been successfully used in Japan and partly in Europe (Table 2) [21, 32, 33••]. This cross-calibration of H/M ratio enables a better comparison between institutions and unifies H/M ratios among various institutions in multicenter studies, which is important for identifying appropriate thresholds for differentiating high- and low-risk patients.

The Diagnostic and Prognostic Role of Cardiac ^{123}I-*m*IBG Imaging

Since its introduction, cardiac ^{123}I-*m*IBG imaging has been shown to be an important predictor for many cardiac diseases. Although most cardiac ^{123}I-*m*IBG imaging studies evaluated chronic heart failure (CHF) populations, there is also evidence that cardiac ^{123}I-*m*IBG imaging has a prognostic role in other cardiac diseases, such as atrial fibrillation, hypertrophic cardiomyopathy, and chemotherapy-induced cardiac toxicity. Cardiac ^{123}I-*m*IBG imaging seems also helpful in the diagnosis for some neurology diseases. This paragraph will discuss the role of cardiac ^{123}I-*m*IBG imaging in cardiac diseases with a focus on CHF. Furthermore, its role as a diagnostic tool in neurology will be discussed.

Cardiac ^{123}I-*m*IBG Imaging in CHF

Since the first study [15] in the early 1990s, a number of small prospective and retrospective studies have confirmed that myocardial ^{123}I-*m*IBG parameters in CHF patients are independent predictors of cardiac events (i.e., progression of HF, arrhythmia, and cardiac death) [14, 34–36]. Patients with impaired myocardial ^{123}I-*m*IBG parameters (i.e., reduced late H/M ratio and increased ^{123}I-*m*IBG WO) had a worse prognosis compared with those with relatively preserved parameters. In 2010, the ADMIRE-HF study, a large prospective multicenter study, confirmed the prognostic value of cardiac ^{123}I-*m*IBG scintigraphy [30]. This study included 961 CHF patients with New York Heart Association

Table 2. Typical conversion coefficients and examples of thresholds for the most used collimator types in clinical practice.

Collimator	Conversion coefficient	H/M = 1.6* with LEHR collimator	H/M = 2.2* with MEGP collimator
LEHR	0.55	**1.60**	1.75
LEGP	0.60	1.65	1.82
LME	0.83	1.91	2.13
MEGP	0.88	1.96	**2.20**
MELP	0.90	1.98	2.23

LEHR, low-energy, high-resolution collimator; *MEGP*, medium-energy general purpose collimator. Thresholds of 1.6 and 2.2 are derived from ADMIRE-HF [30••] and Japanese multicenter study of dementia with Lewy bodies [31], respectively.

(NYHA) functional class II or III HF, LVEF ≤ 35%, and optimized medical therapy (OMT). Late H/M ratio, as a dichotomous variable with a predefined cut-off of 1.6 using a LEHR collimator, was a prognostic predictor independent from other markers, such as brain natriuretic peptide (BNP) and LVEF. The risk of event occurrence was significantly higher in patients with late H/M < 1.6, with a 2-year event rate of 38% ($p < 0.001$). Moreover, the 2-year death rate, whether cardiac or all-cause, decreased linearly with increased late H/M ratio, dropping from 20% with late H/M ratio < 1.1 to none with late H/M ratio ≥ 1.8. Since the ADMIRE-HF study, a late H/M ratio cut-off of 1.6 became an accepted cut-off to discriminate low- and high-risk patients. However, this cut-off point is based on LEHR collimator use only. Therefore, for institutions using other types of collimators than a LEHR collimator, the cut-off value should be corrected using the above described cross-calibration phantom [21, 32, 33] (Table 2). A meta-analyses including individual patient and original image data of 636 CHF patients retrieved from 6 studies from USA and Europe showed that the late H/M ratio is not only useful as a dichotomous predictor of events (i.e., high vs. low risk) but also has prognostic implication over the full range of the outcome value for all event categories except ventricular arrhythmias [37••]. The latter is interesting as there are also some smaller studies suggesting an association between increased cardiac sympathetic activity and arrhythmic events or appropriate implantable cardioverter defibrillator (ICD) therapy [38–40]. In a prospective study including 116 CHF patients, eligible for ICD implantation for both primary and secondary prevention of sudden cardiac death (SCD), ^{123}I-*m*IBG SPECT was shown to be an independent predictor of appropriate ICD therapy and cardiac death [39]. The cumulative incidence of appropriate ICD therapy during 3-year follow-up was significantly higher when a relatively large ^{123}I-*m*IBG SPECT defect (median summed defect score (SDS) > 26) was present. In another small study including 27 CHF patients referred for ICD implantation patients with fatal arrhythmia and SCD had lower late H/M ratios and higher ^{123}I-*m*IBG SPECT SDS compared to those without an arrhythmic event [38]. Except from these small studies, a (linear) relation between ^{123}I-*m*IBG scintigraphy findings and the occurrence of fatal arrhythmic events is lacking. One explanation could be the heterogeneity of the studied populations including ischemic vs. non-ischemic HF and primary vs. secondary prophylactic ICD implantation.

Currently, there is an international effort to better understand the relation between cardiac ^{123}I-*m*IBG findings and the occurrence of fatal arrhythmic events. Cardiac sympathetic hyperactivity is an important factor in the occurrence of ventricular arrhythmias in patients with a reduced LVEF. In these patients, ventricular arrhythmias develop in relation to enhanced automaticity, triggered automaticity, and re-entrant mechanisms. These mechanisms are enhanced by release of NE [41]. In addition, non-uniform denervated myocardium in infarct tissue can be hypersensitive to NE. Especially the border zone of infarct tissue with viable myocardial tissue is predisposed to develop re-entrant circuits. This mechanism is most likely triggered by the fact that sympathetic nerve fibers are more susceptible to ischemia than myocytes, thereby causing a disbalance between still viable but partly denervated and normal myocardium [42, 43]. Interestingly, a multicenter study including 135 stable CHF subjects (age 64.5 ± 9.3 years, 79% male, LVEF 25 ± 6%) referred for prophylactic ICD implantation showed that in contrast to the linear correlation between ^{123}I-*m*IBG scintigraphy findings by using standardized H/M ratio and the overall prognosis in CHF, there seems to be a "bell-shape" relation between ^{123}I-*m*IBG scintigraphy findings and the occurrence of appropriate ICD therapy (i.e., fatal arrhythmia) [44••]. Figure 3 shows the combined endpoint (i.e., appropriate ICD therapy, progression of HF, SCD, and death due to terminal HF) in relation to standardized late H/M ratio. Patients with intermediate late H/M ratios (range 1.40–2.10) were more likely to have appropriate ICD therapy compared to patients with low and high late H/M ratios. These findings are in line with previous findings of Agostini et al. [14]. Arrhythmia occurred in CHF patients with an intermediate late H/M ratio between 1.46 and 2.17. In addition, Travin et al. concluded that the presumption of a monotonic increase in risk of an arrhythmic event with increasing ^{123}I-*m*IBG SPECT defects may not be correct [45]. This conclusion was based on the observation that in 471 ischemic CHF patients, those with intermediate defects on ^{123}I-*m*IBG SPECT summed score appeared to be at the highest risk for cardiac events. The results of previous studies with a "bell-shaped" curve [14, 44–46] for the late H/M ratio or ^{123}I-*m*IBG SPECT summed score of in relation to ventricular arrhythmia or appropriated ICD therapy underline the previous described hypothesis of the occurrence of ventricular arrhythmias. More importantly, these studies suggest that cardiac ^{123}I-*m*IBG imaging could play a role in patient selection for an expensive disease-modifying therapy such as ICD implantation.

Cardiac resynchronization therapy (CRT) is another disease-modifying therapy in selected CHF patients (QRS ≥ 150 msec, LVEF ≤ 35%, and NYHA class ≥ 2) [47]. However, one-third of these CHF patients does not benefit from CRT. Scholtens et al. reviewed 9 small studies that evaluated CRT and ^{123}I-*m*IBG assessed cardiac innervation [48]. The authors concluded that the lack of uniformity in acquisition protocols, especially collimator use, and the variation in criteria used to define response to CRT impair any direct comparison between the available studies. However, in all available studies, cardiac ^{123}I-*m*IBG scintigraphy showed positive changes in cardiac sympathetic activity in responders to CRT. Furthermore, cardiac ^{123}I-*m*IBG scintigraphy seems to be promising in identifying CHF patients who do not benefit from CRT. This was confirmed

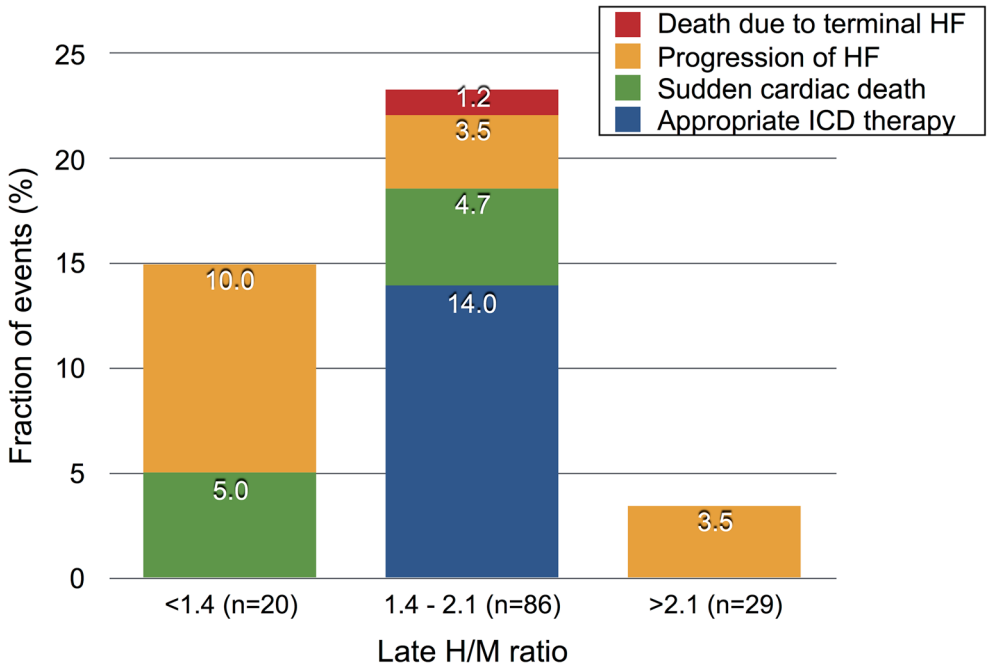

Figure 3. Fraction of combined endpoint (i.e., appropriate ICD therapy, progression of HF, SCD, and death due to terminal HF) per tertile standardized late H/M ratios.

by the single center BETTER-HF study (n = 121) that showed that late H/M ratio was an independent predictor of CRT response defined as LV remodelling with 15% reduction of LVESV (regression coefficient 2.906, 95% CI 0.293–3.903, p = 0.029). However, extrapolation of these data to other institutions is hampered by the lack of uniform CRT response criteria and different collimator use. To overcome the issues of different collimator use, recently, a multicenter study including 78 CHF subjects referred for CRT implantation evaluated cardiac ^{123}I-*m*IBG scintigraphy in relation to response to CRT by using standardized H/M ratio [49]. The results showed that early and late H/M ratios were independent predictors of CRT response when improvement of LVEF was used as measure of response. Therefore, cardiac ^{123}I-*m*IBG scintigraphy maybe used as a tool to selection of subjects that might benefit from CRT.

Cardiac ^{123}I-*m*IBG Imaging in Atrial Fibrillation

Although cardiac ^{123}I-*m*IBG imaging has mainly focussed on CHF, there is also some evidence that cardiac ^{123}I-*m*IBG imaging has prognostic value in subjects with atrial fibrillation. Akutsu et al. showed in 98 patients with idiopathic paroxysmal atrial fibrillation and preserved LVEF (i.e., > 50%) that a lower late H/M ratio (HR 3.44 [CI 1.9–6.2], $p < 0.0001$) and lower LVEF (HR 1.04 [CI 1.01–1.08], p = 0.014) were the independent predictors of the transit from paroxysmal atrial fibrillation to permanent paroxysmal atrial fibrillation [50]. This finding further stresses the relation between autonomic imbalances and the occurrence of arrhythmias.

Cardiac ^{123}I-*m*IBG Imaging in Hypertrophic Cardiomyopathy

Since the introduction of cardiac ^{123}I-*m*IBG imaging, it has been demonstrated that cardiac sympathetic activity is impaired in hypertrophic cardiomyopathy (HCM). Not only serum levels of NE are increased [51–53], but also late H/M ratio is decreased and ^{123}I-*m*IBG WO is increased [54–56]. Some of these studies demonstrated that ^{123}I-*m*IBG WO correlates with the severity of myocardial hypertrophy [54, 55]. Pace et al. evaluated in patients with HCM (n = 11) late H/M ratio and ^{123}I-*m*IBG WO in relation to LVEF and perfusion [57]. ^{123}I-*m*IBG WO showed a positive relation with LVOT obstruction (r = 0.84, $p < 0.001$) and septum thickness (r = 0.76, $p < 0.01$), suggesting that cardiac sympathetic activity correlates to the degree of septal hypertrophy and consequently LVOT obstruction in HCM. Furthermore, late H/M ratio increases and ^{123}I-*m*IBG WO decreases in the months following septal ablation which results in LVOT obstruction reduction [58]. In patients with HCM, congestive HF as a result of LV dilatation and dysfunction is an important predictor of SCD [59–61]. However, clinical tools for predicting the onset of CHF in HCM are limited. A small study including 84 HCM patients demonstrated that cardiac ^{123}I-*m*IBG imaging could be useful in predicting the onset of congested HF in these patients [62]. During a follow-up of 9–86 months, the prevalence of HF was 0% in patients with late H/M ratio > 2.11, 3.3% in patients with late H/M ratio 1.86–2.11, and 55.0% in patients with late H/M ratio < 1.86. Multivariate

analysis showed that late H/M ratio and LV fractional shortening were significant predictors of congested HF in HCM.

Cardiac ^{123}I-*m*IBG Imaging in Oncology Cardiotoxicity

Chemotherapy-related cardiac dysfunction is one of the most notorious side effects of anticancer treatment, occurring in approximately 10% of patients [63]. Anthracyclines are the cornerstone in the treatment of numerous hematological and solid tumors. In a large meta-analysis pooling data from 18 studies involving almost 50,000 patients treated with anthracyclines, the incidence of clinically overt and subclinical cardiotoxicity was reported in 6.3% and 17.9% of patients, respectively [64]. Mechanisms for development of cardiotoxicity involved may include free radicals, myocyte death due to calcium overload, and altered adrenergic function. Dos Santos et al. evaluated in 89 patients the late cardiotoxic effect of anthracyclines by assessing sympathetic activity with cardiac imaging [65]. Although patients treated with anthracyclines had a reduction in LVEF compared to controls, there was no difference in ^{123}I-*m*IBG-derived parameters. However, cardiac ^{123}I-*m*IBG imaging seems sensitive enough to detect alterations in innervation before left ventricular dysfunction occurs. Another study evaluated the correlation between ^{123}I-*m*IBG assessed cardiac sympathetic activity and echocardiography assessed global longitudinal strain (GLS), global radial strain, (GRS) and biomarkers [66]. The parameters found as the most robust were late H/M ratio and ^{123}I-*m*IBG WO. Nevertheless, it is important to emphasize that there was a significant correlation between H/M ratio and GRS.

All these preliminary data suggest that it seems feasible to assess cardiotoxicity with cardiac ^{123}I-*m*IBG imaging. Furthermore, cardiac ^{123}I-*m*IBG imaging in combination with parameters of LV impairment seems to be promising for routine clinical use in these oncology patients.

Cardiac ^{123}I-*m*IBG Imaging in Specific Neurology Diseases

To understand the pathophysiology in different neurogenerative diseases, cardiac ^{123}I-*m*IBG imaging has been useful. Spinocerebellar ataxia type 2 (SCA2) is an autosomal dominant neurogenerative disorder with often autonomic nervous system dysfunction. Cardiac ^{123}I-*m*IBG imaging revealed that compared to Parkinson's disease, the cardiac innervation in SCA2 is less impaired [67]. Huntington's disease (HD) is also an autosomal dominant neurodegenerative disorder with potential cardiac manifestation of severe autonomic dysfunction, including tachycardia, arrhythmia, and SCD. Recently, Assante et al. demonstrated that ^{123}I-*m*IBG assessed cardiac innervation was preserved in patients with HD, suggesting that cardiovascular dysfunction might be mainly due to impairment of brain areas associated with the regulation and modulation of the heart function [68].

Not only is cardiac ^{123}I-*m*IBG imaging helpful in better understanding the pathophysiology of some neurodegenerative diseases, but it is also useful in daily clinical practice. Reduced cardiac uptake in ^{123}I-*m*IBG scintigraphy is considered as a biomarker of Lewy body diseases including dementia with Lewy bodies, Parkinson's disease, and pure autonomic failure [69–71]. The diagnostic thresholds for late H/M ratio were reported as 2.2 (standardized to the ME collimator condition) for dementia with Lewy bodies [31] and 1.77 (not standardized) for Lewy body diseases including Parkinson's disease (see Table 2 for conversion) [72]. In Japan, cardiac ^{123}I-*m*IBG scintigraphy was approved and reimbursed for any cardiac diseases since 1992, and additionally approved by social insurance for Parkinson's disease and dementia with Lewy bodies in 2012 [20]. Total number of all cardiac SPECT imaging is around 250,000 per year and the number reached plateau or slightly decreased currently. However, in contrast to USA and Europe, the number of cardiac ^{123}I-*m*IBG scintigraphy is increasing in Japan and reached approximately 50,000 studies per year, in which 2/3 are estimated to be performed for neurology purposes (Figure 4). Although ^{123}I-Ioflupane has been approved worldwide for Parkinson's disease, parkinsonism, and dementia, the indications of ^{123}I-Ioflupane are mainly for the differentiation of neurodegenerative and non-neurodegenerative such as essential tremor and drug-induced parkinsonism. Cardiac ^{123}I-*m*IBG imaging can differentiate Parkinson's disease from various types of Parkinson's syndrome, whereas activity is decreased on images of both Parkinson's diseases and syndrome with ^{123}I-Ioflupane. Therefore, it has been recognized that clinical roles for diagnosis are different between ^{123}I-*m*IBG and ^{123}I-Ioflupane. Although the role of imaging might be limited for patients with typical neurological symptoms and signs, the ability to accurately diagnose borderline cases remains a challenge even for neurologists. Whether such clinical experiences of combined use of ^{123}I-*m*IBG and ^{123}I-Ioflupane for neurodegenerative diseases and dementia can be extrapolated to other countries need to be further investigated. However, the practical role of cardiac ^{123}I-*m*IBG imaging for neurology purposes should be emphasized.

Risk Models Using Cardiac ^{123}I-*m*IBG Imaging

CHF is the only cardiovascular disease with both growing incidence and prevalence [73]. As a consequence, the medical costs for HF will increase. Therefore, there is a need for more precise patient-tailored risk stratification in order to achieve a more (cost)effective management of patients with CHF. To enhance the utility of risk markers, a large number of scintigramultivariate risk models have been developed in the

past decades [74–77]. However, the clinical use of these models remains limited. Based on a multicenter Japanese cohort study (n = 933), a risk model was developed for predicting 5-year cardiac mortality in CHF patients [78]. Parameters used in this model include age, gender, NYHA functional class, and LVEF. By adding late H/M ratio to the net reclassification improvement, analysis for all subjects was 13.8% ($p < 0.0001$) and its inclusion was most effective in the downward reclassification of low-risk patients. Based on 2- and 5-year risk models using 4 variables (NYHA class, age, LVEF, and late H/M ratio), mortality risk charts for CHF patients have been developed [79•].

Recently, a redefined risk model using machine learning has been developed for predicting 2 years risk of life-threatening arrhythmia and HF death [80•]. In total, 13 variables were used including age, gender, NYHA functional class, LVEF, and late H/M ratio. An example is shown in Figure 5. The probability of HF death significantly increased as late H/M ratio decreased when variables were combined. However, the probability of arrhythmic events was maximal when late H/M ratio was intermediate. This is in line with previously described studies showing a "bell-shaped" curve of arrhythmic events in relation to ^{123}I-*m*IBG-derived parameters [44–46]. Furthermore, cardiac ^{123}I-*m*IBG scintigraphy for a better selection of ICD candidates seems to be cost-effective [81]. In a cost-effectiveness model, screening was associated with a reduction in ICD implantation by 21%, resulting in a number needed to screen to prevent 1 ICD implantation of 5. Consequently, costs per patient were reduced by US$5500 and US$13,431 over 2 and 10 years, respectively, in comparison with no screening. Use of cardiac ^{123}I-*m*IBG scintigraphy screening resulted in losses of 0.001 and 0.040 life-years, respectively, over 2 and 10 years. These findings are encouraging in better discriminating those who benefit from those who do not benefit from ICD implantation. However, larger studies are necessary to further define the role of cardiac ^{123}I-*m*IBG imaging in patient selection for ICD implantation.

Why Has Cardiac ^{123}I-*m*IBG Imaging not Fulfilled Its Clinical Potential?

Many factors contribute to the eventual success (or failure) of a new nuclear imaging agent. Among these are the following: the quality of the efficacy evidence, including the ability to confirm the new findings using existing established methods; widespread availability of the agent from commercial suppliers; ease of use of the agent with existing imaging equipment; and price in relation to levels of reimbursement from government and private insurers. While early evaluations of many new diagnostic radiopharmaceuticals are in small investigator-initiated studies, commercialization typically requires larger, sponsored multicenter trials to support submissions to pharmaceutical regulatory agencies for marketing approval in various countries. This latter process, which is often both lengthy and expensive, sometimes results in judgment errors that adversely affect one or more of the success factors noted above.

It is instructive to compare the early time courses of cardiac ^{123}I-*m*IBG imaging in oncology and cardiology, considering that the initial work in both areas occurred at about the same time. Although both early ^{123}I-*m*IBG imaging oncology and cardiology studies were investigator-designed and executed, the former benefited from meeting an unmet medical need for a reliable diagnostic procedure for rare neural crest tumors such as pheochromocytoma and neuroblastoma [2, 82]. In cardiology, although the physiological association between myocardial ^{123}I-*m*IBG uptake and NET-mediated sympathetic neuron function was established in early studies [83, 84], there was neither a direct anatomical correlate for the new imaging findings nor a specific therapeutic action that could be taken in response. While ^{123}I-*m*IBG imaging

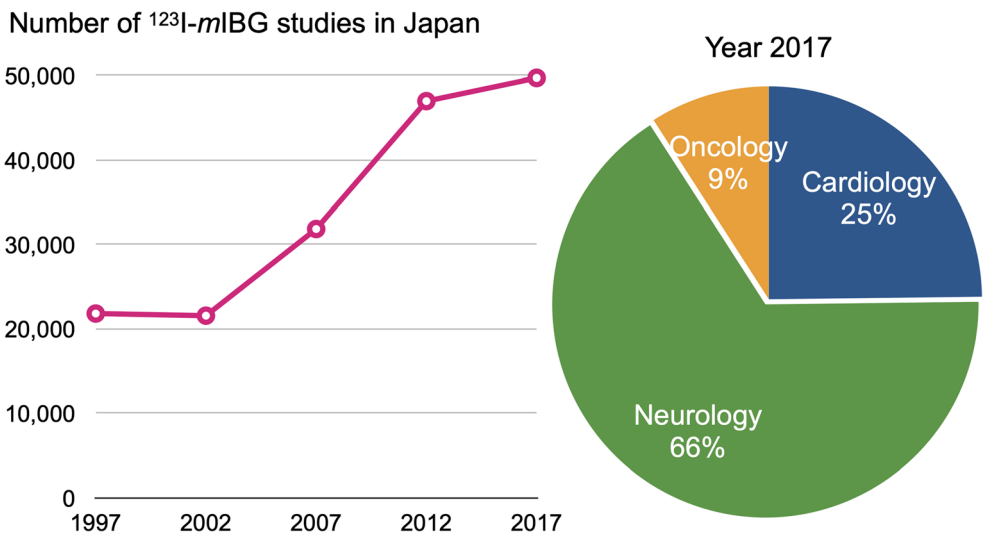

Figure 4. Number of cardiac ^{123}I-*m*IBG studies in Japan and fraction of clinical applications.

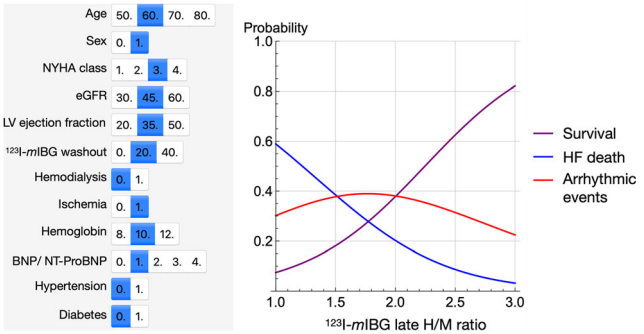

Figure 5. An example of the probability of HF death, arrhythmia, and survival (no events) for 60-year-old male with NYHA class III and LVEF 35%. The selected conditions of the variables are shown in blue. The probability of events is plotted as a function of late ^{123}I-*m*IBG H/M ratio. The probabilities were calculated by a three-category classifier.

results were being used by oncologists in the mid-1980s in clinical management of patients with pheochromocytoma and neuroblastoma, cardiologists considered ^{123}I-*m*IBG findings interesting but of uncertain utility.

During the past 30 years, hundreds of studies using cardiac ^{123}I-*m*IBG imaging, both planar and SPECT, have been published [20, 85]. Three broad categories of studies, diagnostic, response to therapy, and prognostic, are of particular relevance to the degree of clinical utilization of the procedure.

Analogous to most other diagnostic radiopharmaceuticals (including ^{123}I-*m*IBG for oncology), the most consistent growth area for ^{123}I-*m*IBG cardiology use has been as a diagnostic agent. In both Europe and Japan, the majority of cardiac ^{123}I-*m*IBG imaging studies are performed for evaluation of patients with neurologic disorders such as Parkinson's disease and Lewy body disease, which can cause extensive cardiac dysinnervation. The high sensitivity and specificity of a simple discrimination between preserved and significantly decreased cardiac innervation is the primary reason cardiac ^{123}I-*m*IBG imaging has been incorporated into clinical practice [86, 87]. The irony is that it is usually neurologists, not cardiologists, who order the study. In the USA, where ^{123}I-*m*IBG is not indicated for neurological imaging, these procedures are rarely performed.

Neither the numerous studies showing changes in cardiac ^{123}I-*m*IBG imaging findings as a measure of response to heart disease therapy [49, 88] nor the enormous number of outcome studies documenting the prognostic significance of myocardial ^{123}I-*m*IBG uptake in HF and other chronic heart conditions [30, 37, 89, 90] has convinced cardiologists of the value and relevance of the procedure in routine clinical practice. This reflects a fundamental reality in cardiology: in a guidelines-driven field, prognostic information that does not change management is of little value. The difference between a predicted 2% and 10% annual mortality risk may be statistically significant, but if it reflects underlying disease that is already being treated in accordance with current guidelines, the information will be unlikely to change how the cardiologist treats the patient. Even if this same example was converted to risk for SCD in a patient eligible for an ICD, almost all cardiologists would adhere to the guidelines even if ^{123}I-*m*IBG imaging suggested the patient's true arrhythmic event risk was extremely low [90]. Currently, there are no randomized clinical trials that demonstrated that cardiac ^{123}I-*m*IBG-guided therapy improves CHF patient outcomes, and without such data, clinical cardiologists have little incentive to order the scans. There is no substitute for prospective trial data that demonstrates patient benefit from the information provided by the diagnostic imaging procedure.

In recent years, clinical use of cardiac ^{123}I-*m*IBG imaging has also been affected by the perception that the method is outdated in comparison with other technologies. Whether it is the continued reliance on planar imaging and the rudimentary quantitation of the heart/mediastinum ratio in a field now dominated by quantitative tomographic techniques, the limited image quality of even the best ^{123}I-*m*IBG SPECT study compared with PET scans using agents such as ^{11}C-HED [91] or ^{18}F-Flubrobenguane [92], or the advancements in other imaging and invasive cardiac mapping technologies [93, 94], convincing cardiologists to use cardiac ^{123}I-*m*IBG imaging is challenging. Eventual approval of a cardiac PET agent capable of quantifying sympathetic innervation will probably make this challenge even more daunting. Except in locations where ^{123}I-*m*IBG is relatively inexpensive and can be used as a binary diagnostic test agent, it seems unlikely there will be significant growth in ^{123}I-*m*IBG imaging procedure volume in the foreseeable future.

However, given the increasing medical costs associated with HF, a better selection of patients for expensive therapy such as devices (i.e., ICD and CRT) is mandatory. The current selection criteria fail to make a proper selection of patients that benefit from these devices. If there is a potential clinical role for cardiac ^{123}I-*m*IBG imaging in CHF, it will be in guiding the selection of these HF patients. Although currently available data show promising result for cardiac ^{123}I-*m*IBG imaging, none of these studies was designed to demonstrate that ^{123}I-*m*IBG-guided findings can be used to improve patient outcomes (analogous to standard randomized double-blind therapy trials).

Conclusion

Cardiac ^{123}I-*m*IBG imaging is a widely available non-invasive modality to assess cardiac sympathetic activity. Over the past 4 decades, cardiac ^{123}I-*m*IBG imaging has been established to evaluate the prognosis, especially in CHF and diagnosis in specific neurological diseases. Standardization, especially among various gamma camera-collimator combinations, is important for identifying appropriate thresholds for adequate risk stratification. In contrast to the linear relationship between ^{123}I-*m*IBG-derived parameters and the overall prognosis in CHF, there seems a "bell-shape" curve for ^{123}I-*m*IBG-derived parameters and fatal arrhythmias. These new insights could be helpful in

patient selection for expensive therapy such as devices (i.e., ICD and CRT). However, none of the previous studies were designed to demonstrate that ^{123}I-*m*IBG-guided findings can be used to improve patient outcomes. Therefore, except from Japan, cardiac ^{123}I-*m*IBG imaging has not widely been accepted as clinical tool. So, future trials are essential to address this topic and will help in establishing clinical acceptance of the robust non-invasive imaging tool that cardiac ^{123}I-*m*IBG imaging is.

Abbreviations ^{123}I-*m*IBG, ^{123}I-*meta*-iodobenzylguanidine; CHF, Chronic heart failure; CRT, Cardiac resynchronization therapy; ICD, Implantable cardioverter-defibrillator; H/M ratio, Heart-to-mediastinum ratio; LVEF, Left ventricular ejection fraction; MPI, Myocardial perfusion imaging; NE, Norepinephrine; SCD, Sudden cardiac death; WO, Washout

Declarations

Conflict of Interest D.O. Verschure reports personal fees from Astra Zeneca and personal fees from Novartis. A.F. Jacobson was an employee at GE Healthcare during the conduct of the original ADMIRE-HF study. K. Nakajima has collaborative research works with FUJIFILM Toyama Chemical, Co, Ltd, Japan. H.J. Verberne declares that he has no conflict of interest.

References

Papers of particular interest, published recently, have been highlighted as:
- • Of importance
- •• Of major importance

1. Wieland DM, Wu J-l, Brown LE, Mangner TJ, Swanson DP, Beierwaltes WH. Radiolabeled adrenergic neuron-blocking agents: adrenomedullary imaging with [131I] iodobenzylguanidine. J Nucl Med. 1980;21(4):349–53.
2. Wieland DM, Brown LE, Les Rogers W, Worthington KC, Wu JI. Clinthorne NH et al. Myocardial imaging with a radioiodinated norepinephrine storage analog. J Nucl Med. 1981;22(1):22–31.
3. Kline RC, Swanson DP, Wieland DM, Thrall JH, Gross MD, Pitt B, et al. Myocardial imaging in man with I-123 meta-iodobenzylguanidine. J Nucl Med. 1981;22(2):129–32.
4. Manger WM, Hoffman BB. Heart imaging in the diagnosis of pheochromocytoma and assessment of catecholamine uptake. J Nucl Med Off Pub Soc Nuc Med. 1983;24(12):1194–6.
5. Nakajo M, Shapiro B, Glowniak J, Sisson JC, Beierwaltes WH. Inverse relationship between cardiac accumulation of meta-[131I]iodobenzylguanidine (I-131 MIBG) and circulating catecholamines in suspected pheochromocytoma. J Nuc Med Off Pub Soc Nuc Med. 1983;24(12):1127–34.
6. Cohn JN, Levine TB, Olivari MT, Garberg V, Lura D, Francis GS, et al. Plasma norepinephrine as a guide to prognosis in patients with chronic congestive heart failure. N Engl J Med. 1984;311(13):819–23. https://doi.org/10.1056/NEJM198409273111303.
7. Henderson EB, Kahn JK, Corbett JR, Jansen DE, Pippin JJ, Kulkarni P, et al. Abnormal I-123 metaiodobenzylguanidine myocardial washout and distribution may reflect myocardial adrenergic derangement in patients with congestive cardiomyopathy. Circulation. 1988;78(5 Pt 1):1192–9. https://doi.org/10.1161/01.cir.78.5.1192.
8. Schofer J, Spielmann R, Schuchert A, Weber K, Schluter M. Iodine-123 meta-iodobenzylguanidine scintigraphy: a noninvasive method to demonstrate myocardial adrenergic nervous system disintegrity in patients with idiopathic dilated cardiomyopathy. J Am Coll Cardiol. 1988;12(5):1252–8.
9. Tanaka T, Aizawa T, Kato K, Nakano H, Igarashi M, Ueno T, et al. Estimation of myocardial sympathetic neuronal function with I-123 metaiodobenzylguanidine (MIBG) in patients with acute myocardial infarction undergoing percutaneous transluminal coronary thrombolysis (PTCR). Kaku igaku Japanese J Nucl Med. 1988;25(12):1425–9.
10. Hirosawa K, Tanaka T, Hisada K, Bunko H. Clinical evaluation of 123I-MIBG for assessment of the sympathetic nervous system in the heart (multi-center clinical trial). Kaku igaku Japanese J Nucl Med. 1991;28(5):461–76.
11. Glowniak JV, Turner FE, Gray LL, Palac RT, Lagunas-Solar MC, Woodward WR. Iodine-123 metaiodobenzylguanidine imaging of the heart in idiopathic congestive cardiomyopathy and cardiac transplants. J Nucl Med Off Pub Soc Nucl Med. 1989;30(7):1182–91.
12. Richalet JP, Merlet P, Bourguignon M, Le-Trong JL, Kéromès A, Rathat C, et al. MIBG scintigraphic assessment of cardiac adrenergic activity in response to altitude hypoxia. J Nucl Med Off Pub Soc Nucl Med. 1990;31(1):34–7.
13. Grötz J, Franitza R, Mödder G, Hossmann V. Scintigraphic imaging of adrenergic structures of the heart with 123(I)-metaiodobenzylguanidine in cardiomyopathy. Z Kardiol. 1988;77(5):278–81.
14. Agostini D, Verberne HJ, Burchert W, Knuuti J, Povinec P, Sambuceti G, et al. I-123-mIBG myocardial imaging for assessment of risk for a major cardiac event in heart failure patients: insights from a retrospective European multicenter study. Eur J Nucl Med Mol Imaging. 2008;35(3):535–46. https://doi.org/10.1007/s00259-007-0639-3.
15. Merlet P, Valette H, Dubois-Randé JL, Moyse D, Duboc D, Dove P, et al. Prognostic value of cardiac metaiodobenzylguanidine imaging in patients with heart failure. J Nucl Med Off Pub Soc Nucl Med. 1992;33(4):471–7.
16. Verschure DO, Bongers V, Hagen P, Somsen GA, van Eck-Smit BF, Verberne H. Impact of a predefined mediastinal ROI on inter-observer variability of planar 123I-MIBG heart-to-mediastinum ratio. J Nucl Cardiol. 2014;21(3):605–13. https://doi.org/10.1007/s12350-014-9854-z.
17. Pellegrino T, Petretta M, De Luca S, Paolillo S, Boemio A, Carotenuto R, et al. Observer reproducibility of results from a low-dose 123I-metaiodobenzylguanidine cardiac imaging protocol in patients with heart failure. Eur J Nucl Med Mol Imaging. 2013;40(10):1549–57. https://doi.org/10.1007/s00259-013-2461-4.
18. Veltman C, Boogers M, Meinardi J, Al Younis I, Dibbets-Schneider P, Van der Wall E, et al. Reproducibility of planar 123I-meta-iodobenzylguanidine (MIBG) myocardial scintigraphy in patients with

heart failure. Eur J Nucl Med Mol Imaging. 2012;39(10):1599–608. https://doi.org/10.1007/s00259-012-2180-2.

19.•• Flotats A, Carrió I, Agostini D, Le Guludec D, Marcassa C, Schaffers M, et al. Proposal for standardization of 123I-metaiodobenzylguanidine (MIBG) cardiac sympathetic imaging by the EANM Cardiovascular Committee and the European Council of Nuclear Cardiology. Eur J Nucl Med Mol Imaging. 2010;37(9):1802–12. https://doi.org/10.1007/s00259-010-1491-4 **The authors of this paper provide essential information about standardization of ^{123}I-*m*IBG cardiac imaging.**

20. Travin MI, Matsunari I, Thomas GS, Nakajima K, Yoshinaga K. How do we establish cardiac sympathetic nervous system imaging with (123)I-mIBG in clinical practice? Perspectives and lessons from Japan and the US. J Nucl Cardiology Off Pub Am Soc Nucl Cardiology. 2019;26(4):1434–51. https://doi.org/10.1007/s12350-018-1394-5.

21. Okuda K, Nakajima K, Kitamura C, Kirihara Y, Hashimoto M, Kinuya S. Calibrated scintigraphic imaging procedures improve quantitative assessment of the cardiac sympathetic nerve activity. Sci Rep. 2020;10(1):21834. https://doi.org/10.1038/s41598-020-78917-8.

22. Nakajima K, Matsumoto N, Kasai T, Matsuo S, Kiso K, Okuda K. Normal values and standardization of parameters in nuclear cardiology: Japanese Society of Nuclear Medicine working group database. Ann Nucl Med. 2016;30(3):188–99. https://doi.org/10.1007/s12149-016-1065-z.

23. Nakajima K, Okuda K, Matsuo S, Wakabayashi H, Kinuya S. Is (123)I-metaiodobenzylguanidine heart-to-mediastinum ratio dependent on age? From Japanese Society of Nuclear Medicine normal database. Ann Nucl Med. 2018;32(3):175–81. https://doi.org/10.1007/s12149-018-1231-6.

24. Holly TA, Abbott BG, Al-Mallah M, Calnon DA, Cohen MC, DiFilippo FP, et al. Single photon-emission computed tomography. J Nucl Cardiology Off Pub Am Soc Nucl Cardiology. 2010;17(5):941–73. https://doi.org/10.1007/s12350-010-9246-y.

25. Gimelli A, Liga R, Genovesi D, Giorgetti A, Kusch A, Marzullo P. Association between left ventricular regional sympathetic denervation and mechanical dyssynchrony in phase analysis: a cardiac CZT study. Eur J Nucl Med Mol Imaging. 2014;41(5):946–55. https://doi.org/10.1007/s00259-013-2640-3.

26. Gimelli A, Liga R, Giorgetti A, Genovesi D, Marzullo P. Assessment of myocardial adrenergic innervation with a solid-state dedicated cardiac cadmium-zinc-telluride camera: first clinical experience. Eur Heart J Cardiovasc Imaging. 2014;15(5):575–85. https://doi.org/10.1093/ehjci/jet258.

27. Henzlova MJ, Duvall WL, Einstein AJ, Travin MI, Verberne HJ. ASNC imaging guidelines for SPECT nuclear cardiology procedures: stress, protocols, and tracers. J Nucl Cardiol. 2016;23(6):606–39. https://doi.org/10.1007/s12350-015-0387-x.

28. Okuda K, Nakajima K, Hosoya T, Ishikawa T, Konishi T, Matsubara K, et al. Semi-automated algorithm for calculating heart-to-mediastinum ratio in cardiac Iodine-123 MIBG imaging. J Nucl Cardiology Off Pub Am Soc Nucl Cardiology. 2011;18(1):82–9. https://doi.org/10.1007/s12350-010-9313-4.

29. Verschure DO, de Wit TC, Bongers V, Hagen PJ, Sonneck-Koenne C, D'Aron J, et al. ^{123}I-MIBG heart-to-mediastinum ratio is influenced by high-energy photon penetration of collimator septa from liver and lung activity. Nuclear Med Comm. 2015;36(3):279–85. https://doi.org/10.1097/mnm.0000000000000238.

30.•• Jacobson AF, Senior R, Cerqueira MD, Wong ND, Thomas GS, Lopez VA, et al. Myocardial iodine-123 meta-iodobenzylguanidine imaging and cardiac events in heart failure. Results of the prospective ADMIRE-HF (AdreView Myocardial Imaging for Risk Evaluation in Heart Failure) study. J Am Coll Cardiol. 2010;55(20):2212–21. https://doi.org/10.1016/j.jacc.2010.01.014 **This paper of the ADMIRE-HF study presents results of the first multicenter study that evaluate cardiac ^{123}I-*m*IBG imaging in heart failure.**

31. Komatsu J, Samuraki M, Nakajima K, Arai H, Arai H, Arai T, et al. (123)I-MIBG myocardial scintigraphy for the diagnosis of DLB: a multicentre 3-year follow-up study. J Neurol Neurosurg Psychiatry. 2018;89(11):1167–73. https://doi.org/10.1136/jnnp-2017-317398.

32. Verschure DO, Poel E, Nakajima K, Okuda K, van Eck-Smit BLF, Somsen GA, et al. A European myocardial (123)I-mIBG cross-calibration phantom study. J Nucl Cardiology Off Pub Am Soc Nucl Cardiology. 2018;25(4):1191–7. https://doi.org/10.1007/s12350-017-0782-6.

33.• Nakajima K, Okuda K, Yoshimura M, Matsuo S, Wakabayashi H, Imanishi Y, et al. Multicenter cross-calibration of I-123 metaiodobenzylguanidine heart-to-mediastinum ratios to overcome camera-collimator variations. J Nucl Cardiology Off Pub Am Soc Nucl Cardiology. 2014;21(5):970–8. https://doi.org/10.1007/s12350-014-9916-2 **The authors of this paper provide essential information about standardization H/M ratio for different collimator gamma camera combination.**

34. Merlet P, Benvenuti C, Moyse D, Pouillart F, Dubois-Rande JL, Duval AM, et al. Prognostic value of MIBG imaging in idiopathic dilated cardiomyopathy. J Nucl Med Off Pub Soc Nucl Med. 1999;40(6):917–23.

35. Nakata T, Miyamoto K, Doi A, Sasao H, Wakabayashi T, Kobayashi H, et al. Cardiac death prediction and impaired cardiac sympathetic innervation assessed by MIBG in patients with failing and nonfailing hearts. J Nucl Cardiology Off Pub Am Soc Nucl Cardiology. 1998;5(6):579–90. https://doi.org/10.1016/s1071-3581(98)90112-x.

36. Cohen-Solal A, Esanu Y, Logeart D, Pessione F, Dubois C, Dreyfus G, et al. Cardiac metaiodobenzylguanidine uptake in patients with moderate chronic heart failure: relationship with peak oxygen uptake and prognosis. J Am Coll Cardiol. 1999;33(3):759–66. https://doi.org/10.1016/s0735-1097(98)00608-1.

37.•• Verschure DO, Veltman CE, Manrique A, Somsen GA, Koutelou M, Katsikis A, et al. For what endpoint does myocardial 123I-MIBG scintigraphy have the greatest prognostic value in patients with chronic heart failure? Results of a pooled individual patient data meta-analysis. Eur Heart J Cardiovasc Imaging. 2014;15(9):996–1003. https://doi.org/10.1093/ehjci/jeu044 **This meta-analysis including 636 patients analyzed cardiac ^{123}I-*m*IBG imaging and found that the late H/M ratio is not only useful as a dichotomous predictor of events (high vs. low risk) but also has prognostic implication over the full range of the outcome value for all event categories except arrhythmias.**

38. Marshall A, Cheetham A, George RS, Mason M, Kelion AD. Cardiac iodine-123 metaiodobenzylguanidine imaging predicts ventricular arrhythmia in heart failure patients receiving an implantable cardioverter-defibrillator for primary prevention. Heart. 2012;98(18):1359–65. https://doi.org/10.1136/heartjnl-2012-302321.

39. Boogers MJ, Borleffs CJW, Henneman MM, van Bommel RJ, van Ramshorst J, Boersma E, et al. Cardiac sympathetic denervation assessed with 123-iodine metaiodobenzylguanidine imaging predicts ventricular arrhythmias in implantable cardioverter-defibrillator patients. J Am Coll Cardiol. 2010;55(24):2769–77. https://doi.org/10.1016/j.jacc.2009.12.066.

40. Yamamoto H, Yamada T, Tamaki S, Morita T, Furukawa Y, Iwasaki Y, et al. Prediction of sudden cardiac death in patients with chronic heart failure by regional washout rate in cardiac MIBG SPECT imaging. J Nucl Cardiol. 2019;26(1):109–17. https://doi.org/10.1007/s12350-017-0913-0.

41. Podrid P, Fuchs T, Candinas R. Role of the sympathetic nervous system in the genesis of ventricular arrhythmia. Circulation. 1990;82(2 Suppl):I103–13.

42. Zipes DP. Influence of myocardial ischemia and infarction on autonomic innervation of heart. Circulation. 1990;82(4):1095–105.
43. Matsunari I, Schricke U, Bengel FM, Haase HU, Barthel P, Schmidt G, et al. Extent of cardiac sympathetic neuronal damage is determined by the area of ischemia in patients with acute coronary syndromes. Circulation. 2000;101(22):2579–85.
44.•• Verschure DO, de Groot JR, Mirzaei S, Gheysens O, Nakajima K, van Eck-Smit BLF, et al. Cardiac 123I-mIBG scintigraphy is associated with freedom of appropriate ICD therapy in stable chronic heart failure patients. Int J Cardiol. 2017;248:403–8. https://doi.org/10.1016/j.ijcard.2017.08.003 **This study demonstrated a nonlinear relationship between ^{123}I-*m*IBG imaging and arrhythmia in subjects with CHF.**
45. Travin MI, Henzlova MJ, van Eck-Smit BLF, Jain D, Carrio I, Folks RD, et al. Assessment of (123)I-mIBG and (99m)Tc-tetrofosmin single-photon emission computed tomographic images for the prediction of arrhythmic events in patients with ischemic heart failure: intermediate severity innervation defects are associated with higher arrhythmic risk. J Nucl Cardiology Off Pub Am Soc Nucl Cardiology. 2017;24(2):377–91. https://doi.org/10.1007/s12350-015-0336-8.
46. De Vincentis G, Frantellizzi V, Fedele F, Farcomeni A, Scarparo P, Salvi N, et al. Role of cardiac (123)I-mIBG imaging in predicting arrhythmic events in stable chronic heart failure patients with an ICD. J Nucl Cardiology Off Pub Am Soc Nucl Cardiology. 2018;26:1188–96. https://doi.org/10.1007/s12350-018-1258-z.
47. Ponikowski P, Voors AA, Anker SD, Bueno H, Cleland JG, Coats AJ, et al. 2016 ESC Guidelines for the diagnosis and treatment of acute and chronic heart failure: the Task Force for the diagnosis and treatment of acute and chronic heart failure of the European Society of Cardiology (ESC). Developed with the special contribution of the Heart Failure Association (HFA) of the ESC. Eur J Heart Fail. 2016;18(8):891–975. https://doi.org/10.1002/ejhf.592.
48. Scholtens AM, Braat AJ, Tuinenburg A, Meine M, Verberne HJ. Cardiac sympathetic innervation and cardiac resynchronization therapy. Heart Fail Rev. 2014;19(5):567–73. https://doi.org/10.1007/s10741-013-9400-0.
49. Verschure DO, Poel E, De Vincentis G, Frantellizzi V, Nakajima K, Gheysens O, et al. The relation between cardiac 123I-mIBG scintigraphy and functional response 1 year after CRT implantation. Eur Heart J Cardiovasc Img. 2021;22(1):49–57. https://doi.org/10.1093/ehjci/jeaa045.
50. Akutsu Y, Kaneko K, Kodama Y, Li HL, Suyama J, Shinozuka A, et al. Iodine-123 mIBG imaging for predicting the development of atrial fibrillation. J Am Coll Cardiol Img. 2011;4(1):78–86. https://doi.org/10.1016/j.jcmg.2010.10.005.
51. Li ST, Tack CJ, Fananapazir L, Goldstein DS. Myocardial perfusion and sympathetic innervation in patients with hypertrophic cardiomyopathy. J Am Coll Cardiol. 2000;35(7):1867–73. https://doi.org/10.1016/s0735-1097(00)00626-4.
52. Schäfers M, Dutka D, Rhodes CG, Lammertsma AA, Hermansen F, Schober O, et al. Myocardial presynaptic and postsynaptic autonomic dysfunction in hypertrophic cardiomyopathy. Circ Res. 1998;82(1):57–62. https://doi.org/10.1161/01.res.82.1.57.
53. Brush JE Jr, Eisenhofer G, Garty M, Stull R, Maron BJ, Cannon RO 3rd, et al. Cardiac norepinephrine kinetics in hypertrophic cardiomyopathy. Circulation. 1989;79(4):836–44. https://doi.org/10.1161/01.cir.79.4.836.
54. Nakajima K, Bunko H, Taki J, Shimizu M, Muramori A, Hisada K. Quantitative analysis of 123I-meta-iodobenzylguanidine (MIBG) uptake in hypertrophic cardiomyopathy. Am Heart J. 1990;119(6):1329–37. https://doi.org/10.1016/s0002-8703(05)80183-8.
55. Taki J, Nakajima K, Bunko H, Simizu M, Muramori A, Hisada K. Whole-body distribution of iodine 123 metaiodobenzylguanidine in hypertrophic cardiomyopathy: significance of its washout from the heart. Eur J Nucl Med. 1990;17(5):264–8. https://doi.org/10.1007/bf00812368.
56. Shimizu M, Sugihara N, Kita Y, Shimizu K, Horita Y, Nakajima K, et al. Long-term course and cardiac sympathetic nerve activity in patients with hypertrophic cardiomyopathy. Br Heart J. 1992;67(2):155–60. https://doi.org/10.1136/hrt.67.2.155.
57. Pace L, Betocchi S, Losi MA, Della Morte AM, Ciampi Q, Nugnez R, et al. Sympathetic nervous function in patients with hypertrophic cardiomyopathy assessed by [123I]-MIBG: relationship with left ventricular perfusion and function. The quarterly journal of nuclear medicine and molecular imaging : official publication of the Italian Association of Nuclear Medicine (AIMN) [and] the International Association of Radiopharmacology (IAR), [and] Section of the So. 2004;48(1):20–5.
58. Okayama S, Uemura S, Horii M, Kawata H, Saito Y. Continuing improvement of cardiac sympathetic activity on I-123 MIBG scintigraphy in a patient with hypertrophic obstructive cardiomyopathy after percutaneous transluminal septal myocardial ablation. J Nucl Cardiology Off Pub Am Soc Nucl Cardiology. 2008;15(5):e31–4. https://doi.org/10.1016/j.nuclcard.2008.06.015.
59. Spirito P, Maron BJ, Bonow RO, Epstein SE. Occurrence and significance of progressive left ventricular wall thinning and relative cavity dilatation in hypertrophic cardiomyopathy. Am J Cardiol. 1987;60(1):123–9. https://doi.org/10.1016/0002-9149(87)90998-2.
60. McKenna W, Deanfield J, Faruqui A, England D, Oakley C, Goodwin J. Prognosis in hypertrophic cardiomyopathy: role of age and clinical, electrocardiographic and hemodynamic features. Am J Cardiol. 1981;47(3):532–8. https://doi.org/10.1016/0002-9149(81)90535-x.
61. ten Cate FJ, Roelandt J. Progression to left ventricular dilatation in patients with hypertrophic obstructive cardiomyopathy. Am Heart J. 1979;97(6):762–5. https://doi.org/10.1016/0002-8703(79)90012-7.
62. Hiasa G, Hamada M, Saeki H, Ogimoto A, Ohtsuka T, Hara Y, et al. Cardiac sympathetic nerve activity can detect congestive heart failure sensitively in patients with hypertrophic cardiomyopathy. Chest. 2004;126(3):679–86. https://doi.org/10.1378/chest.126.3.679.
63. Cardinale D, Colombo A, Bacchiani G, Tedeschi I, Meroni CA, Veglia F, et al. Early detection of anthracycline cardiotoxicity and improvement with heart failure therapy. Circulation. 2015;131(22):1981–8. https://doi.org/10.1161/circulationaha.114.013777.
64. Lotrionte M, Biondi-Zoccai G, Abbate A, Lanzetta G, D'Ascenzo F, Malavasi V, et al. Review and meta-analysis of incidence and clinical predictors of anthracycline cardiotoxicity. Am J Cardiol. 2013;112(12):1980–4. https://doi.org/10.1016/j.amjcard.2013.08.026.
65. Dos Santos MJ, da Rocha ET, Verberne HJ, da Silva ET, Aragon DC, Junior JS. Assessment of late anthracycline-induced cardiotoxicity by (123)I-mIBG cardiac scintigraphy in patients treated during childhood and adolescence. J Nucl Cardiology Off Pub Am Soc Nucl Cardiology. 2017;24(1):256–64. https://doi.org/10.1007/s12350-015-0309-y.
66. Bulten BF, Verberne HJ, Bellersen L, Oyen WJ, Sabaté-Llobera A, Mavinkurve-Groothuis AM, et al. Relationship of promising methods in the detection of anthracycline-induced cardiotoxicity in breast cancer patients. Cancer Chemother Pharmacol. 2015;76(5):957–67. https://doi.org/10.1007/s00280-015-2874-9.

67. De Rosa A, Pappatà S, Pellegrino T, De Leva MF, Maddaluno G, Fiumara G, et al. Reduced cardiac 123I-metaiodobenzylguanidine uptake in patients with spinocerebellar ataxia type 2: a comparative study with Parkinson's disease. Eur J Nucl Med Mol Imaging. 2013;40(12):1914–21. https://doi.org/10.1007/s00259-013-2524-6.
68. Assante R, Salvatore E, Nappi C, Peluso S, De Simini G, Di Maio L, et al. Autonomic disorders and myocardial 123I-metaiodobenzylguanidine scintigraphy in Huntington's disease. J Nucl Cardiology Off Pub Am Soc Nucl Cardiology. 2020. https://doi.org/10.1007/s12350-020-02299-7.
69. Orimo S, Suzuki M, Inaba A, Mizusawa H. 123I-MIBG myocardial scintigraphy for differentiating Parkinson's disease from other neurodegenerative parkinsonism: a systematic review and meta-analysis. Parkinsonism Relat Disord. 2012;18(5):494–500. https://doi.org/10.1016/j.parkreldis.2012.01.009.
70. McKeith IG, Boeve BF, Dickson DW, Halliday G, Taylor JP, Weintraub D, et al. Diagnosis and management of dementia with Lewy bodies: fourth consensus report of the DLB Consortium. Neurology. 2017;89(1):88–100. https://doi.org/10.1212/wnl.0000000000004058.
71. Nakajima K, Yamada M. (123)I-Meta-iodobenzylguanidine sympathetic imaging: standardization and application to neurological diseases. Chonnam Med J. 2016;52(3):145–50. https://doi.org/10.4068/cmj.2016.52.3.145.
72. King AE, Mintz J, Royall DR. Meta-analysis of 123I-MIBG cardiac scintigraphy for the diagnosis of Lewy body-related disorders. Off J Move Dis Soc. 2011;26(7):1218–24. https://doi.org/10.1002/mds.23659.
73. Okura Y, Ramadan MM, Ohno Y, Mitsuma W, Tanaka K, Ito M, et al. Impending epidemic: future projection of heart failure in Japan to the year 2055. Off J Japanese Circ Soc. 2008;72(3):489–91. https://doi.org/10.1253/circj.72.489.
74. Pocock SJ, Ariti CA, McMurray JJ, Maggioni A, Køber L, Squire IB, et al. Predicting survival in heart failure: a risk score based on 39 372 patients from 30 studies. Eur Heart J. 2013;34(19):1404–13. https://doi.org/10.1093/eurheartj/ehs337.
75. Levy WC, Mozaffarian D, Linker DT, Sutradhar SC, Anker SD, Cropp AB, et al. The Seattle Heart Failure Model: prediction of survival in heart failure. Circulation. 2006;113(11):1424–33. https://doi.org/10.1161/circulationaha.105.584102.
76. Sartipy U, Dahlström U, Edner M, Lund LH. Predicting survival in heart failure: validation of the MAGGIC heart failure risk score in 51,043 patients from the Swedish heart failure registry. Eur J Heart Fail. 2014;16(2):173–9. https://doi.org/10.1111/ejhf.32.
77. O'Connor CM, Whellan DJ, Wojdyla D, Leifer E, Clare RM, Ellis SJ, et al. Factors related to morbidity and mortality in patients with chronic heart failure with systolic dysfunction: the HF-ACTION predictive risk score model. Circ Heart Fail. 2012;5(1):63–71. https://doi.org/10.1161/circheartfailure.111.963462.
78. Nakajima K, Nakata T, Yamada T, Yamashina S, Momose M, Kasama S, et al. A prediction model for 5-year cardiac mortality in patients with chronic heart failure using (1)(2)(3)I-metaiodobenzylguanidine imaging. Eur J Nucl Med Mol Imaging. 2014;41(9):1673–82. https://doi.org/10.1007/s00259-014-2759-x.
79.• Nakajima K, Nakata T, Matsuo S, Jacobson AF. Creation of mortality risk charts using 123I meta-iodobenzylguanidine heart-to-mediastinum ratio in patients with heart failure: 2- and 5-year risk models. Europe Heart J Cardiovascular Img. 2016;17(10):1138–45. https://doi.org/10.1093/ehjci/jev322 **The authors of this paper provide essential information about the usefulness of cardiac ^{123}I-*m*IBG imaging in risk calculation.**
80.• Nakajima K, Nakata T, Doi T, Tada H, Maruyama K. Machine learning-based risk model using (123)I-metaiodobenzylguanidine to differentially predict modes of cardiac death in heart failure. J Nucl Cardiology Offi Pub Am Soc Nucl Cardiology. 2020. https://doi.org/10.1007/s12350-020-02173-6 **The authors of this paper provide essential information about machine learning and cardiac ^{123}I-*m*IBG imaging in risk calculation.**
81. O'Day K, Levy WC, Johnson M, Jacobson AF. Cost-effectiveness analysis of iodine-123 meta-iodobenzylguanidine imaging for screening heart failure patients eligible for an implantable cardioverter defibrillator in the USA. App Health Econ Health policy. 2016;14(3):361–73. https://doi.org/10.1007/s40258-016-0234-5.
82. Shapiro B, Sisson JC, Shulkin BL, Gross MD, Zempel S. The current status of meta-iodobenzylguanidine and related agents for the diagnosis of neuro-endocrine tumors. The quarterly journal of nuclear medicine : official publication of the Italian Association of Nuclear Medicine (AIMN) [and] the International Association of Radiopharmacology (IAR). 1995;39(4 Suppl 1):3–8.
83. Tobes MC, Jaques S Jr, Wieland DM, Sisson JC. Effect of uptake-one inhibitors on the uptake of norepinephrine and metaiodobenzylguanidine. J Nucl Med Off Pub Soc Nucl Med. 1985;26(8):897–907.
84. Jaques S Jr, Tobes MC, Sisson JC, Baker JA, Wieland DM. Comparison of the sodium dependency of uptake of metalodobenzylguanidine and norepinephrine into cultured bovine adrenomedullary cells. Mol Pharmacol. 1984;26(3):539–46.
85. Wan N, Travin MI. Cardiac imaging with (123)I-meta-iodobenzylguanidine and analogous PET tracers: current status and future perspectives. Semin Nucl Med. 2020;50(4):331–48. https://doi.org/10.1053/j.semnuclmed.2020.03.001.
86. Treglia G, Cason E, Stefanelli A, Cocciolillo F, Di Giuda D, Fagioli G, et al. MIBG scintigraphy in differential diagnosis of Parkinsonism: a meta-analysis. Clin Auto Res Off J Clin Auto Res Soc. 2012;22(1):43–55. https://doi.org/10.1007/s10286-011-0135-5.
87. Frantellizzi V, Lavelli V, Ferrari C, Sardaro A, Farcomeni A, Pacilio M, et al. Diagnostic value of the early heart-to-mediastinum count ratio in cardiac 123I-mIBG imaging for Parkinson's disease. Curr Radiopharm. 2020;14:64–9. https://doi.org/10.2174/1874471013999200727211633.
88. Kasama S, Toyama T, Hatori T, Sumino H, Kumakura H, Takayama Y, et al. Evaluation of cardiac sympathetic nerve activity and left ventricular remodelling in patients with dilated cardiomyopathy on the treatment containing carvedilol. Eur Heart J. 2007;28(8):989–95. https://doi.org/10.1093/eurheartj/ehm048.
89. Nakata T, Nakajima K, Yamashina S, Yamada T, Momose M, Kasama S, et al. A pooled analysis of multicenter cohort studies of (123)I-mIBG imaging of sympathetic innervation for assessment of long-term prognosis in heart failure. J Am Coll Cardiol Img. 2013;6(7):772–84. https://doi.org/10.1016/j.jcmg.2013.02.007.
90. Narula J, Gerson M, Thomas GS, Cerqueira MD, Jacobson AF. (1)(2)(3)I-MIBG imaging for prediction of mortality and potentially fatal events in heart failure: the ADMIRE-HFX study. J Nucl Med Off Pub Soc Nucl Med. 2015;56(7):1011–8. https://doi.org/10.2967/jnumed.115.156406.
91. Fallavollita JA, Heavey BM, Luisi AJ Jr, Michalek SM, Baldwa S, Mashtare TL Jr, et al. Regional myocardial sympathetic denervation predicts the risk of sudden cardiac arrest in ischemic cardiomyopathy. J Am Coll Cardiol. 2014;63(2):141–9. https://doi.org/10.1016/j.jacc.2013.07.096.
92. Sinusas AJ, Lazewatsky J, Brunetti J, Heller G, Srivastava A, Liu YH, et al. Biodistribution and radiation dosimetry of LMI1195:

first-in-human study of a novel 18F-labeled tracer for imaging myocardial innervation. J Nucl Med Off Pub Soc Nucl Med. 2014;55(9):1445–51. https://doi.org/10.2967/jnumed.114.140137.

93. Klein T, Abdulghani M, Smith M, Huang R, Asoglu R, Remo BF, et al. Three-dimensional 123I-meta-iodobenzylguanidine cardiac innervation maps to assess substrate and successful ablation sites for ventricular tachycardia: feasibility study for a novel paradigm of innervation imaging. Circ Arrhythm Electrophysiol. 2015;8(3):583–91. https://doi.org/10.1161/circep.114.002105.
94. Imanli H, Ume KL, Jeudy J, Bob-Manuel T, Smith MF, Chen W, et al. Ventricular tachycardia (VT) substrate characteristics: insights from multimodality structural and functional imaging of the VT substrate using cardiac MRI scar, (123)I-metaiodobenzylguanidine SPECT innervation, and bipolar voltage. J Nucl Med Off Pub Soc Nucl Med. 2019;60(1):79–85. https://doi.org/10.2967/jnumed.118.211698.